Climate drivers of malaria seasonality and their relative importance in Sub-Saharan Africa

Edmund Ilimoan Yamba[1], Andreas H. Fink[2], Kingsley Badu[3], Ernest Ohene Asare[4], Adrian Mark Tompkins[5], and Leonard K Amekudzi[6]

[1]Department of Meteorology and Climate Science, Kwame Nkrumah University of Science and Technology (KNUST)
[2]Karlsruhe Institute of Technology
[3]Kwame Nkrumah University of Science and Technology
[4]Yale School of Public Health
[5]Abdus Salam International Centre for Theoretical Physics (ICTP)
[6]Department of Physics, Kwame Nkrumah University of Science and Technology (KNUST), Kumasi-Ghana

November 26, 2022

Abstract

A new database of the Entomological Inoculation Rate (EIR) is used to directly link the risk of infectious mosquito bites to climate in Sub-Saharan Africa. Applying a statistical mixed model framework to high-quality monthly EIR measurements collected from field campaigns in Sub-Saharan Africa, we analyzed the impact of rainfall and temperature seasonality on EIR seasonality and determined important climate drivers of malaria seasonality across varied climate settings in the region. We observed that seasonal malaria transmission requires a temperature window of 15-40 degrees Celsius and is sustained if average temperature is well above the minimum or below the maximum temperature threshold. Our study also observed that monthly maximum rainfall for seasonal malaria transmission should not exceed 600 mm in west Central Africa, and 400 mm in the Sahel, Guinea Savannah and East Africa. Based on a multi-regression model approach, rainfall and temperature seasonality were significantly associated with malaria seasonality in most parts of Sub-Saharan Africa except in west Central Africa. However, areas characterized by significant elevations such as East Africa, topography has a significant influence on which climate variable is an important determinant of malaria seasonality. Malaria seasonality lags behind rainfall seasonality only at markedly seasonal rainfall areas such as Sahel and East Africa; elsewhere, malaria transmission is year-round. The study's outcome is important for the improvement and validation of weather-driven dynamical malaria models that directly simulate EIR. It can contribute to the development of malaria models fit-for-purpose to support health decision-making towards malaria control or elimination in Sub-Saharan Africa.

Climate drivers of malaria transmission seasonality and their relative importance in Sub-Saharan Africa

Edmund I. Yamba[1], Andreas H. Fink[2], Kingsley Badu[3], Ernest O. Asare[4]Adrian M. Tompkins[5]and Leonard K. Amekudzi[1]

[1]Department of Meteorology and Climate Science, Kwame Nkrumah University of Science and Technology (KNUST), Kumasi-Ghana

[2]Institute of Meteorology and Climate Research, Karlsruhe Institute of Technology, Karlsruhe, Germany

[3]Department of Theoretical and Applied Biology, Kwame Nkrumah University of Science and Technology, Kumasi, Ghana

[4]Department of Epidemiology of Microbial Diseases, Yale School of Public Health, Yale University, New Haven, CT, USA

[5]International Centre for Theoretical Physics, Earth System Physics, Trieste, Italy

Key Points:

- Seasonal malaria transmission in Sub-Saharan Africa is sustained at temperatures well above 15°C or below 40°C.
- Monthly maximum rainfall for seasonal malaria transmission should not exceed 600 mm.
- Rainfall and temperature are significant drivers of malaria seasonality in all parts of Sub-Saharan Africa except in west Central Africa.
- Topography has significant influence on which climate variable is an important driver of malaria seasonality in East Africa.
- Malaria transmission onset lags behind rainfall only at markedly seasonal rainfall areas, otherwise, malaria transmission is year-round.

Corresponding author: Edmund I. Yamba, `eyilimoan48@gmail.com`

Abstract

A new database of the Entomological Inoculation Rate (EIR) is used to directly link the risk of infectious mosquito bites to climate in Sub-Saharan Africa. Applying a statistical mixed model framework to high-quality monthly EIR measurements collected from field campaigns in Sub-Saharan Africa, we analyzed the impact of rainfall and temperature seasonality on EIR seasonality and determined important climate drivers of malaria seasonality across varied climate settings in the region. We observed that seasonal malaria transmission was within a temperature window of 15°C – 40°C and was sustained if average temperature was well above 15°C or below 40°C. Monthly maximum rainfall for seasonal malaria transmission did not exceed 600 mm in west Central Africa, and 400 mm in the Sahel, Guinea Savannah and East Africa. Based on a multi-regression model approach, rainfall and temperature seasonality were found to be significantly associated with malaria seasonality in all parts of Sub-Saharan Africa except in west Central Africa. Topography was found to have significant influence on which climate variable is an important determinant of malaria seasonality in East Africa. Seasonal malaria transmission onset lags behind rainfall only at markedly seasonal rainfall areas such as Sahel and East Africa; elsewhere, malaria transmission is year-round. High-quality EIR measurements can usefully supplement established metrics for seasonal malaria. The study's outcome is important for the improvement and validation of weather-driven dynamical mathematical malaria models that directly simulate EIR. Our results can contribute to the development of malaria models fit-for-purpose to support health decision-making in the fight to control or eliminate malaria in Sub-Saharan Africa.

1 Introduction

Sub-Saharan Africa remains the world's region with the greatest malaria burden despite massive efforts over the past decades to lower or eliminate malaria (WHO, 2020). Though poor health care systems and low socio-economic status (Degarege et al., 2019; Yadav et al., 2014) are contributing factors, the climate suitability of the region for malaria transmission has a major influence (Caminade et al., 2014). Generally, climate variables such as temperature, rainfall and relative humidity are known to have significant influence on the development and survival of both the malaria parasites and their vectors. Malaria parasite development is not possible at temperatures below 16°C and temperatures above 40°C have adverse effect on mosquito population turnover (Parham and Michael, 2010; Mordecai et al., 2013; Blanford et al., 2013; Shapiro et al., 2017). Rainfall provides the environment for vector breeding (Ermert et al., 2011; Tompkins and Ermert, 2013; Kar et al., 2014) and relative humidity of at least 60% appears necessary for vector survival (Thompson et al., 2005). Rainfall therefore affects the availability, persistence and dimensions of Anopheles vectors and their larval habitats (Fournet et al., 2010; Afrane et al., 2012a; Boyce et al., 2016; Asare et al., 2016a). Previous work studying the relationship between sporozoite development and the survival of infectious mosquitoes found optimal temperatures for efficient malaria transmission between 25°C and 27°C (Bayoh, 2001; Lunde et al., 2013a,b). In Sub-Saharan Africa, most countries have annual mean temperatures between 20°C and 28°C (Lunde et al., 2013a). Given Sub-Saharan Africa's warm tropical climate, a plethora of efficient and effective malaria parasite and vectors thrives in this setting (Sinka et al., 2010; Murray et al., 2012). Understanding the relative importance of climate drivers of malaria seasonality is crucial for describing the geographic patterns of the heterogeneous risk and burden of malaria across the sub-region (Gething et al., 2011; Reiner et al., 2015). This could translate to substantial public health gains, taking into account the seasonality in malaria control and prevention interventions, by helping to determine when, where and how to apply vector and parasite control measures.

To our knowledge, there are insufficient field studies using Entomological Inoculation Rate (EIR, defined as the number of infectious mosquito bites person receives per time) data to relate climate to malaria seasonality in Sub-Saharan Africa. Mabaso et al. (2007) assessed the relationship between EIR seasonality and environmental variables in Africa using a rainfall seasonality index (Markham, 1970). The index fails to capture seasonality at areas with bimodal rainfall regimes, however. Furthermore, the study did not take into consideration the impact of diverse climatic conditions on seasonality outcomes but aggregated data from sites of different climate and environmental settings into a single study, which has the potential to skew the results. Other research has examined the link between malaria and climate variables but primarily relied on clinical data or malaria suitability indices (Lowe et al., 2013; Midekisa et al., 2015; Komen et al., 2015). Both malaria indices and case data have drawbacks for studying malaria seasonality.

Malaria indices are derived using statistical relationships between weather and malaria measures and their out-of-sample generalization over space and time for seasonality studies is subject to significant uncertainties. Clinical case data are also subject to significant uncertainties due to the inaccurate diagnostics (often counts of suspected cases, with temporal inconsistency in the use of Rapid Diagnostic Test, RDT or slide analysis) and under-counting due to varying health-seeking behaviour and health policies (Afrane et al., 2012b). Given that the biology of the malaria parasite and its vector mosquito are temperature and rainfall dependent (Ermert et al., 2011), and that EIR can directly quantify parasite-infected mosquitoes and their propensity to transmit the parasites to humans (MARA, 1998; Shaukat et al., 2010) or estimate the seasonality of the exposure of a population to malaria parasite inoculations (Beier et al., 1999; Takken and Lindsay, 2003), then EIR should be able to usefully relate climate to malaria seasonality better than malaria cases.

In this study, therefore, we investigated the impact of climate variables on EIR seasonality in diverse climate settings across Sub-Saharan Africa with the goal of identifying significant climate determinants of malaria seasonality, their relative importance and variability across the region. To our knowledge, this is the first study to use $\mathrm{EIR_m}$ to explore the impact of climatic variables on malaria seasonality in Sub-Saharan Africa on this wider scale. We applied a mixed model statistiacal framework to a high-quality malaria EIR data (Yamba et al., 2018; Yamba et al., 2020) gathered from publicly available field campaigns of sufficient duration and determined the climate effect that explained significant variations in EIR seasonality. Our findings are intended to provide an understanding of geographical heterogeneous malaria risk from climate effect and support future malaria modeling and forecasting efforts. It will contribute to the development of malaria models especially weather-driven dynamical malaria models fit-for-purpose to support health decision-making in the fight to control or eliminate malaria in Sub-Saharan Africa.

2 Data and Methods

2.1 Study Area

The study area includes locations in Sub-Saharan Africa (as shown in Figure 1), where mosquitoes have previously been collected for malariometrics such as Human Biting Rate (HBR), CircumSporozoite Protein Rates (CSPR), and EIR. The geographical coordinates and elevation of each location are detailed in Tables S1 to S4. The study locations are grouped into four distinct climate zones namely Sahel, Guinea, WCA, and EA (see Figure 1). Each zone has a unique climate conditions from others (see Figure S1) and therefore have different climate implications on malaria seasonality (Yamba, 2016). The division into zones is, therefore, to ensure that malaria transmission patterns are consistent across geographical areas with similar climate characteristics. The seasonal distribution of rainfall

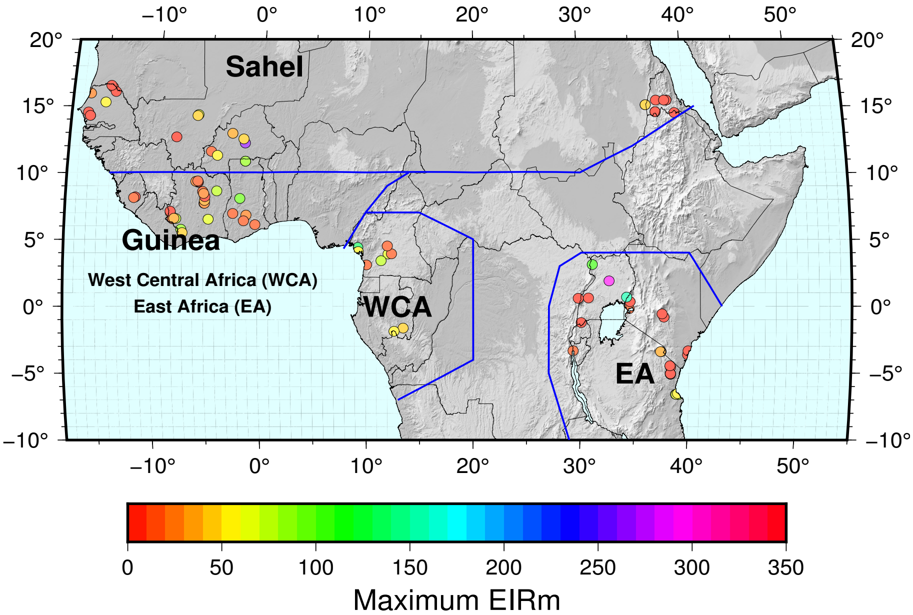

Figure 1: The map of the Sub-Saharan Africa showing field survey sites for EIR. The colour gradient of each site show the maximum EIR available. The blue lines delineate the region into climate zones of Sahel, Guinea, WCA and EA.

and temperature for each zone is shown in Figure S1. In the Sahel, rainfall is markedly seasonal, with a single wet season (usually June to October) and a protracted dry season (November to May). Seasonal temperature ranges between a minimum value of 20 ^{o}C during the harmattan season and to a maximum of about 40 ^{o}C during the pre-monsoon season. In general, temperatures are higher in the Sahel and colder in EA due to the fact that most areas are characterized by higher altitudes.

2.2 Data

2.2.1 Monthly EIR data

Monthly malaria EIR data (hereafter referred to as $\mathrm{EIR_m}$) were obtained from a newly compiled and published monthly malaria EIR database (Yamba et al., 2018; Yamba et al., 2020) for each study location shown in Figure 1. The years and months for which the $\mathrm{EIR_m}$ data were available for each study location is shown in Table S1-S4. Generally, most locations had 12 months of data while other locations had data varying between 24 and 36 months. The data also spanned the period 1983-2013 for all locations. The temporal duration of the data is mostly limited to one year because sampling mosquitoes for EIR is extremely capital and labour intensive (Kilama et al., 2014; Tusting et al., 2014; Badu et al., 2013). The EIR database from which data were extracted for use in this work is a comprehensive one. It was constructed through an all-inclusive literature review using google scholar and PubMed search facilities. All data in that database was generated from publicly available field campaigns of adequate duration and is freely available for public usage in the PANGAEA repository (Yamba et al., 2018). Details of how this database was constructed including compilation, sources, recording, spatial coverage and temporal resolutions are clearly described in Yamba et al. (2020).

2.2.2 Meteorological data

Monthly rainfall (RR) and temperature (minimum (T_{min}), mean (T_{mean}) and maximum (T_{max})) data for each study location were gathered. Rainfall data was obtained from the Global Precipitation Climatology Centre (GPCC) product, version 2018 (Schneider et al., 2018). The GPCC data is a gridded gauge-analysis products and available globally from 1891-2016 at a spatial resolution of 0.25°. GPCC was chosen because it is a rain gauge-analysis product built from quality-controlled rainfall data from ground-based weather stations. Previous validation studies (Manzanas et al., 2014; Atiah et al., 2020) have also found it to be reliable and consistent with ground-based weather observations. The temperature data was obtained from the European Centre for Medium-Range Weather Forecasts (ECMWF) Re-Analysis, 5th generation (ERA5) (Hersbach et al., 2020). ERA5 is also a gridded re-analysis product and available globally on an hourly time scale from 1979 to present at a high spatial resolution of 0.25° by 0.25°. ERA5 was chosen because previous evaluation studies of the product (Tarek et al., 2020; Gleixner et al., 2020; Oses et al., 2020) have widely recommended it for meteorological research. RR, T_{min} and T_{max} were extracted from the respective database for each study location using the nearest grid point of the location's geographical coordinates. T_{mean} values were estimated by averaging the T_{min} and T_{max} values for the location. The extracted temperature and rainfall data had to also conform with the exact years and months at which EIR_m data were available for each location. The study relied on GPCC and ERA5 because, ground-based local weather stations from which these data could be gathered were mostly not available at the EIR sites or, if present, often have sparse data.

2.3 Data analysis

The analysis was conducted for each classified zone as shown in Fig 1. EIR data from locations characterized with the presence of permanent water bodies and/or irrigation activities were exempted. Irrigation and permanent water bodies (such as damps, rivers, streams, swamps etc) have significant influence on the intensity and length of seasonal malaria transmission (Ermert et al., 2011; Tompkins and Ermert, 2013; Asare et al., 2016b; Asare and Amekudzi, 2017). Their exclusion was, therefore, a means to dissociate the influence of these hydrological parameters on malaria seasonality and reducing the impact to climate factors alone.

2.3.1 pair-wise comparison

The study examined the ranges of RR, $\mathrm{T_{min}}$, $\mathrm{T_{mean}}$ and $\mathrm{T_{max}}$ at which $\mathrm{EIR_m}$ occurred using a simple pair-wise comparison approach. This was done by first aggregating the $\mathrm{EIR_m}$ data from all locations within each zone into a single time series of 12 months irrespective of the year of availability. Similarly, the corresponding RR, $\mathrm{T_{min}}$, $\mathrm{T_{mean}}$ and $\mathrm{T_{max}}$ data were also aggregated. The aggregated monthly timeseries of RR, $\mathrm{T_{min}}$, $\mathrm{T_{mean}}$, $\mathrm{T_{max}}$ and $\mathrm{EIR_m}$ were then matched head-to-head as shown in Figure 2. The ranges of RR, $\mathrm{T_{min}}$, $\mathrm{T_{mean}}$ and $\mathrm{T_{max}}$ at which EIR occurred were then determined for each zone .

2.3.2 Relative importance of climate predictors

The relative importance of RR, $\mathrm{T_{min}}$, $\mathrm{T_{mean}}$ and $\mathrm{T_{max}}$ in predicting $\mathrm{EIR_m}$ for each climate zone was analysed using a multiple regression model of the form:

$$EIR_{\mathrm{m}} \sim RR + T_{\mathrm{max}} + T_{\mathrm{min}} + T_{\mathrm{mean}} \tag{1}$$

where $\mathrm{EIR_m}$ is the response variable and RR, $\mathrm{T_{min}}$, $\mathrm{T_{mean}}$ and $\mathrm{T_{max}}$ are the predictors. The contribution of each individual predictor to $\mathrm{EIR_m}$ outcome was then quantified (see Table 1 and 2). Each regressor's contribution was considered as the R^2 from univariate regression, and all univariate R^2 values add up to the full model R^2 (Grömping, 2007). The R package "relaimpo" (Grömping, 2007) was utilized for the calculation of the contribution of the reqressors in the model. It implements six different metrics for assessing relative importance of regressors namely:first, last, pratt, betasg, lmg and pmvd. Among these, lmg and pmvd are computer intensive and has advantage over others in the sense that they decompose R^2 into non-negative contributions that automatically sum to the total R^2

(Grömping, 2007). In this study, lmg was invoked since pmvd is patent protected. The lmg calculates the relative contribution of each predictor to the R^2 with the consideration of the sequence of predictors appearing in the model. It intuitively decomposes the total R^2 by adding the predictors to the regression model sequentially. Then, the increased R^2 is considered as the contribution by the predictor just added. The following are mathematical descriptions of lmg metric referenced from Grömping (2007):
For a model with regressors in set S, the R^2 is given as:

$$R^2(S) = \frac{ModelSS(modelwithregressorsinS)}{TotalSS} \tag{2}$$

To add regressors in set M to a model with the regressors in set S, the additional R^2 is given as:

$$seqR^2(M|S) = R^2(MUS) - R^2(S) \tag{3}$$

where the order of the regressors is a permutation of the available regressors $x_1, ..., x_\mathrm{p}$ denoted by the tuple of indices $r = (r_1, ..., r_\mathrm{p})$. Let $S_\mathrm{k}(r)$ denote the set of regressors entered into the model before regressor x_k in the order r. Then the portion of R^2 allocated to regressor x_k in the order r can be written as:

$$seqR^2(\{x_\mathrm{k}\}|S_\mathrm{k}(r)) = R^2(\{x_\mathrm{k}\}US_\mathrm{k}(r)) - R^2(S_\mathrm{k}(r)) \tag{4}$$

With eq. 4, the metric lmg (in formulae denoted as LMG) can be written as:

$$LMG(x_\mathrm{k}) = \frac{1}{P!} \sum_{rpermutation} seqR^2(\{x_\mathrm{k}\}|r) \tag{5}$$

Orders with the same $S_\mathrm{k}(r) = S$ can be summarized into one summand, which simplifies the formula into:

$$LMG(x_\mathrm{k}) = \frac{1}{p!} \sum_{S \subseteq \{x_1,....,x_\mathrm{p}\} \backslash \{x_\mathrm{k}\}} seqR^2(\{x_\mathrm{k}\}|S) \tag{6}$$

The analysis also assessed the relative importance of each regressor (in eqn 1) by looking at what each regressor alone is able to explain (i.e., comparing the R^2 value of regression model with one regressor only without considering the dependence of others as is the case of the metric *lmg*). The metric *first* in the "relaimpo" package was invoked for this purpose because, unlike *lmg*, it is completely ignorant of the other regressors in the model and so no adjustment takes place (Grömping, 2007). Since *first* does not decompose R^2 into contributions like *lmg*), the contribution of the individual regressors alone do not naturally add up to the overall R^2. The sum of these individual contributions is often far higher than the overall R^2 of the model with all regressors together.

Whether *lmg* or *first*, each metric's outcome were bootstrapped to ensure that the relative importance of each regressor was clearly defined (i.e. those different and those that are similar in terms of relative importance). Bootstrapping in "relaimpo" was done using the function boot in the package. Prior to calculating the *lmg* and *first* metrics, all data series (i.e. EIR_m, RR, T_{min}, T_{mean} and T_{max} timeseries) were log transformed. The essence of the log transformation was to decrease the variabilities in the data pairs and make them conform more closely to normal distribution with similar variance and standard deviation (Curran-Everett, 2018).

2.3.3 EIR lag behind rainfall

Seasonal malaria transmission onset lags behind rainfall season onset because of the time taken for mosquito breeding and vector population growth after rainfall season onset (Tompkins and Ermert, 2013; Badu et al., 2013; Asare and Amekudzi, 2017). This lag time as influenced by climate and whether it varies from one climate zone to another is not known. In this analysis, we quantified this lag time for each climate zone using a cross-correlation statistics performed between RR and EIR_m data pairs. In this statistics, RR was treated as the predictor variable and the corresponding EIR_m as the response variable. The pairs were then cross-correlated at lags of -5 to 0 months and the correlation co-efficient at each lag was calculated. The lag with the strongest positive correlation coefficients was identified as the optimum period of delay between rainfall onset and the EIR season for the zone.

3 Results

3.1 pair-wise comparison

Figure 2 shows the EIR_m response ranges of pairs of rainfall (RR) and temperature (T_{min}, T_{mean} and T_{max}). In the Sahel, maximum rainfall (RR) ranges were about 400 mm per month. Temperature ranges generally varied between 20°C – 40°C in this zone. T_{max} ranges were clustered between 25°C – 40°C, T_{min} within 20°C – 30°C and T_{mean} observed within 25°C – 35°C. In Guinea, RR ranges were also centered around 400 mm per month. Temperature response ranges were mostly observed within 25°C – 35°C for T_{max}, 20°C – 25°C for T_{min} and 24°C – 30°C for T_{mean}. In WCA, maximum RR ranges were centered at about 600 mm per month, which is higher compared to ranges observed in the Sahel, Guinea and EA. Temperature response ranges in this zone were slightly lower than observed in the

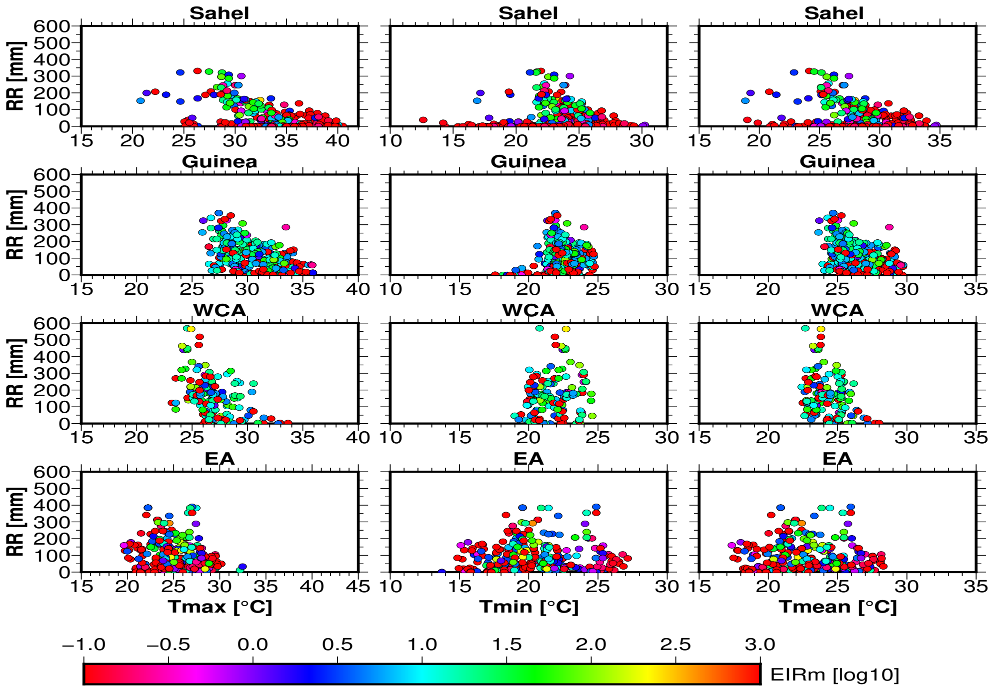

Figure 2: A pair-wise comparison showing the ranges of RR, T_{min}, T_{mean} and T_{max} at which EIR_m occurs. The coloured circles shows log transformed EIR_m values.

Sahel and Guinea. These include 24°C – 32°C for T_{max}, 20°C – 25°C for T_{min} and 22°C – 27°C for T_{mean}. The EA maximum RR ranges were also about 400mm. Temperature ranges of 20°C – 30°C for T_{max}, 15°C – 27°C for T_{min} and 18°C – 29°C for T_{mean} were observed.

3.2 Relative importance of climate predictors

In Table 1 and 2, the relative importance of climate variables in predicting EIR_m is presented for locations with elevations $\leq$ 500 m and > 1000 m respectively. The predictors with p-value ≤ 0.05 were considered significant and interpreted that the respective climate variable significantly predicted the EIR seasonality in that zone. At lower elevations ($\leq$ 500 m) in Sahel, rainfall and temperature were all significant drivers of EIR seasonality cumulatively contributing about 30.72% of the variations in EIR seasonality. At these lower elevation areas, important predictors of EIR_m seasonality were RR and T_{max}. At higher elevations (> 1000 m), rainfall and temperature are together responsible for about 40% of the variations in EIR_m with insignificant contribution from T_{min}. Like the Sahel, temperature and rainfall

Table 1: **The relative contribution of RR, T_{min}, T_{mean} and T_{max} in predicting EIR_m** bootstrapped at confidence interval of 95% for locations with elevations $\leq$ 500 m. Variables with significant p-values contributions are boldfaced. R^2 represents the total proportion of variance in EIR explained by all the climate predictors. lmg values show the individual contribution of each predictor to R^2 relative to others. *First* is the contribution of each predictor alone to R^2 with complete ignorance of the others.

Zone	R^2 [%]	Variable	lmg [%]	First [%]	Coefficient (R)	P-value
Sahel	**30.72**	**RR**	**7.73**	**15.76**	0.3497	**0.0000**
		$\mathbf{T_{max}}$	**12.03**	**17.54**	-15.7276	**0.0000**
		T_{min}	4.89	1.79	3.6380	0.0138
		$\mathbf{T_{mean}}$	**6.07**	**3.20**	-6.8674	**0.0033**
Guinea	**13.59**	**RR**	**5.85**	**10.22**	0.4848	**0.0000**
		$\mathbf{T_{max}}$	**4.09**	**9.65**	-13.3808	**0.0000**
		T_{min}	0.64	0.19	2.7410	0.3760
		$\mathbf{T_{mean}}$	**3.01**	**6.38**	-15.7753	**0.0000**
WCA	**1.69**	RR	0.34	0.23	0.0974	0.5550
		T_{max}	0.60	0.95	5.4640	0.3770
		T_{min}	0.42	0.49	-4.5700	0.5810
		T_{mean}	0.33	0.35	6.8450	0.5280
EA	**31.83**	RR	0.62	0.00	-0.0141	0.9360
		$\mathbf{T_{max}}$	**10.23**	**26.50**	-23.2210	**0.0000**
		$\mathbf{T_{min}}$	**8.84**	**20.10**	-12.1120	**0.0000**
		$\mathbf{T_{mean}}$	**12.14**	**26.04**	-18.2160	**0.0000**

were also significant determinants of EIR_m at lower elevations ($\leq$ 500 m) in Guinea just that their contribution to EIR_m variations is small (about 13.59%) compared to that of Sahel (about 30.72%). In Guinea, also, EIR_m data were unavailable for locations > 1000 m for further analysis in this regard. In WCA, rainfall and temperature were insignificantly associated with EIR_m seasonality whether a lower or higher elevations. Their percentage explanation of the variation in EIR_m were also low (extremely low at lower elevation areas and slighly higher for higher elevation areas) compared to other climate zones. In EA,

Table 2: **Same as Table 1 but for locations with elevations > 1000 m**. In Guinea, EIR data were unavailable for locations at this elevation hence represented as dashed lines.

Zone	R^2 [%]	Variable	lmg [%]	First [%]	Coefficient (R)	P-value
Sahel	40.47	**RR**	7.43	**14.83**	0.3745	**0.0780**
		$\mathbf{T_{max}}$	**17.66**	**35.91**	-10.8070	**0.0036**
		T_{min}	3.69	4.17	-1.4543	0.5950
		$\mathbf{T_{mean}}$	**11.69**	**23.40**	-7.7660	**0.0513**
Guinea	-	RR	-	-	-	-
		T_{max}	-	-	-	-
		T_{min}	-	-	-	-
		T_{mean}	-	-	-	-
WCA	16.55	RR	1.41	1.25	-0.0844	0.7653
		T_{max}	6.70	0.23	6.1700	0.6620
		T_{min}	1.53	0.39	14.1000	0.5970
		T_{mean}	6.91	1.32	12.2800	0.5300
EA	18.22	**RR**	**10.44**	**13.37**	0.5510	**0.0000**
		$\mathbf{T_{max}}$	**1.82**	**3.94**	8.1570	**0.0289**
		$\mathbf{T_{min}}$	**2.88**	**7.77**	10.2080	**0.0011**
		$\mathbf{T_{mean}}$	**3.08**	**6.95**	11.0460	**0.0026**

temperature variables (T_{min}, T_{mean} and T_{max}) were the significant drivers of EIR seasonality at locations ≤ 500 m. It explained about 31% of the seasonality in EIR_m in these areas with extremely insignificant contribution from rainfall. But at areas > 1000 m, all the climate variables were significant contributors with rainfall showing higher contribution to EIR_m variation than temperature.

3.3 EIR lag behind rainfall

Figure 3 shows the seasonal relationship between rainfall and EIR_m (see Figure 3a) and the lag between rainfall onset and EIR onset (see Figure 3b). It is observed in Figure 3a that EIR_m is positively correlated with rainfall. A lag period of 1 month is observed in Sahel

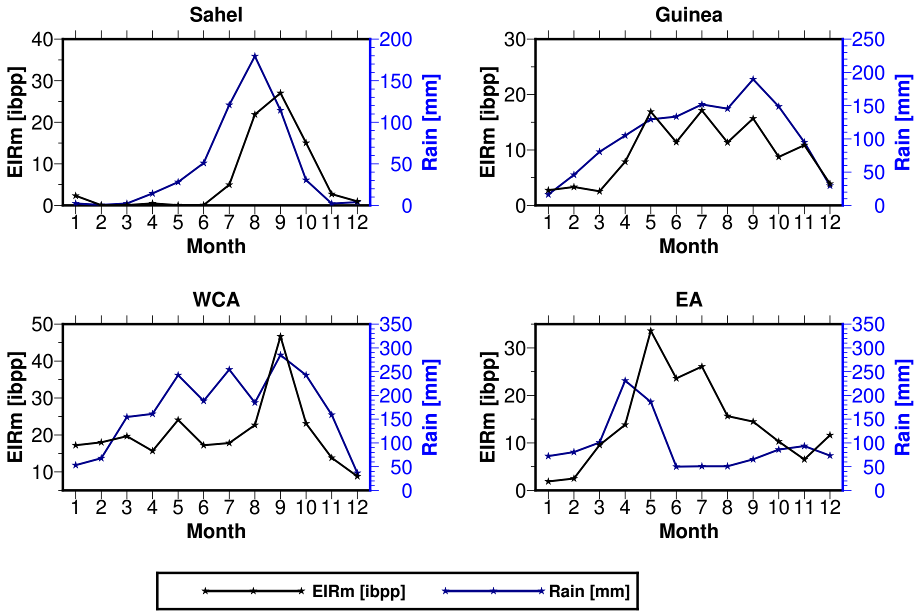

(a) Average monthly time series of EIR_m and rainfall

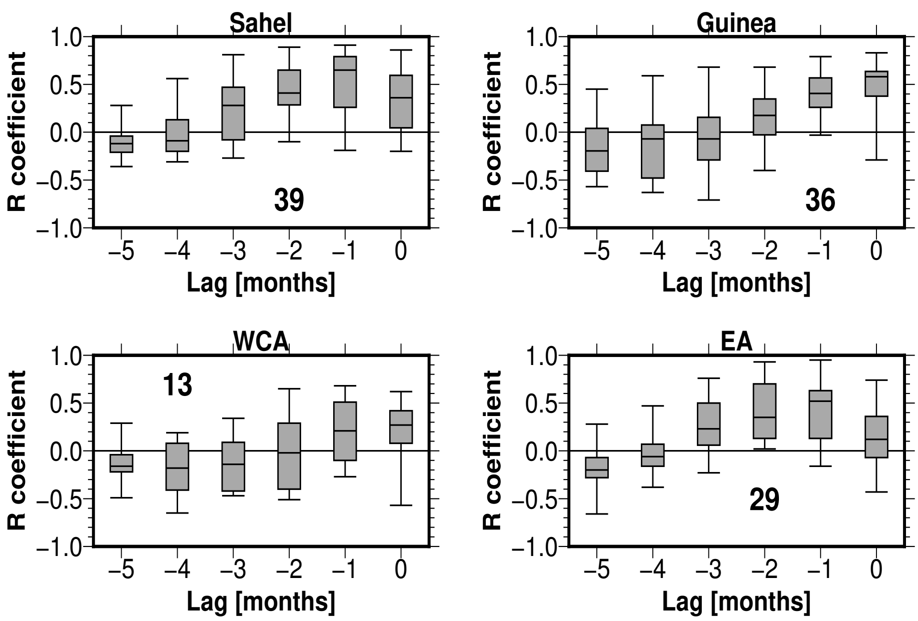

(b) The box-and-whisker plot of cross-correlation coefficient between Rainfall and EIR_m at different lag period

Figure 3: The correlation between rainfall and EIR_m. The numbers 39, 36, 13 and 29 shows the number of location observations contributing to the average timeseries (a) and the box-and-whisker plots (b).

and EA but zero month in Guinea and WCA. Similarly, the cross-correlation statistics determining the lag between the onset of rainy season and the start of the EIR season are shown in Figure 3b. Again, it is observed that the lag at which $\mathrm{EIR_m}$ seasonality strongly and positively correlated with rainfall was 1 month in the Sahel and EA but zero month in Guinea and WCA.

4 Discussion

Our study first examined the seasonal ranges of rainfall and temperature at which $\mathrm{EIR_m}$ occurred in a pair-wise comparison study. In general, temperature ranges of $\mathrm{EIR_m}$ response were mostly clustered between a minimum of 15°C and a maximum of 40°C. This outcome suggests that seasonal malaria transmission is barely impossible below 15°C or above 40°C. Previous studies (Shapiro et al., 2017; Parham and Michael, 2010; Lunde et al., 2013a; Mordecai et al., 2013) have indicated that malaria parasite development is not possible at temperatures below 16°C and that temperatures above 40°C have adverse effect on mosquito population turnover. The outcome of our study using $\mathrm{EIR_m}$ corroborates these previous findings. It provides an additional justification that the number of infectious mosquito bites a person receives per time are associated with changes in temperature. While $\mathrm{T_{min}}$ may be below 16°C as observed in the Sahel and EA (see Figure 2), the daily $\mathrm{T_{mean}}$ must be greater than 16°C particularly for the anopheles mosquitoes for transmission to occur. It should also be significantly less than 40°C for anopheles mosquitoes to survive thermal stress and possible death if seasonal transmission has to take place. Similarly, maximum monthly rainfall values for $\mathrm{EIR_m}$ occurrence was 600 mm in WCA but 400 m in the Sahel, Guinea and EA. The higher monthly maximum rainfall in WCA is due to the fact that annual total rainfall is mostly higher in this region than others (Nicholson, 2013; Froidurot and Diedhiou, 2017). Previous works (Craig et al., 1999; Ermert et al., 2011) have demonstrated that the least monthly amount of rainfall required for malaria transmission is about 80 mm. Our findings suggest that the monthly maximum limit required for seasonal malaria transmission should be about 600 mm in WCA but 400 mm in Sahel, Guinea and EA. Excess of these thresholds could result in flooding of breeding grounds and flushing out and killing the water-bound stage vectors (Paaijmans et al., 2010; Ermert et al., 2011).

The evaluation of the relative importance of RR, $\mathrm{T_{min}}$, $\mathrm{T_{mean}}$ and $\mathrm{T_{max}}$ in predicting EIR seasonality (see details in Table 1 and 2) revealed climate variables that were significantly associated with EIR seasonality in Sub-Saharan Africa. These climate variables are observed as the drivers of malaria seasonality in those zones of the sub-region. The climate variables with highest contribution to EIR variance in each zone are attributed as the most significant drivers. This means that any changes in these significant drivers can result in a substantial changes in malaria seasonality in those areas. Elevation or topography was also observed to play a significant role in determining the important climate drivers of seasonal malaria transmission. In EA for instance, temperature was the important determinant of EIR seasonality at lower elevated areas ($\leq$ 500 m). On the contrary, both rainfall and temperature significantly influenced $\mathrm{EIR_m}$ seasonality at higher elevated areas ($>$1000 m). Though temperature and rainfall are important factors in malaria transmission, our study does not find them to have any significant association with EIR seasonality in WCA. This suggest that malaria seasonality in this zone is importantly driven by other factors other than climate. This require additional studies to unravel these factors driving malaria seasonality in this zone. Mabaso et al. (2007) predicted EIR seasonality from environmental data and found that seasonality in rainfall, minimum temperature, and irrigation were important determinants of seasonality in EIR in Sub-Saharan Africa. Though this study outcome is important, it is not climate specific as it does not justify the implications of diverse climate conditions on EIR seasonality as demonstrated in this study. Other studies (Mabaso et al., 2006; Simple et al., 2018) have used malaria case records from hospitals and found significant correlation between rainfall and temperature. As stated in the introduction, malaria case records have drawbacks for studying malaria seasonality as they are subject to significant uncertainties due to the inaccurate diagnostics and under counting due to varying health-seeking behaviour and health policies (Afrane et al., 2012b).

The cross-correlation statistics showed the lag(s) at which rainfall strongly correlated with $\mathrm{EIR_m}$ in each zone. The lag period suggest the time taken for malaria season to start after rainfall season has started. The lag of 1 month in Sahel and EA signifies that malaria transmission season delays 1 month after the start of rainfall season at these zones. In Guinea and WCA, this lag period was zero month suggesting that there is no delay between rainfall season onset and the start of malaria season. Hence malaria transmission in these zones is year-round. In markedly seasonal rainfall zones such as the Sahel and EA, the delay between rainfall onset and the start of the malaria season is expected. Rainfall in the Sahel is markedly seasonal, lasting from June to October, followed by about six to eight months of dry period (Nicholson, 2013; Froidurot and Diedhiou, 2017). Hence, mosquitoes are barely present during the dry and long hot season. Even if present, they are inactive due to low humidity and high temperature and only recover within the rainy season when rainfall and temperature requirements are suitable. The absence of delay between rainfall season onset and the start of malaria season at Guinea and WCA is also expected. These zones are highly humid with shorter dry seasons (Nicholson, 2013; Froidurot and Diedhiou, 2017). For this reason, vectors are able to persist all year round at these zones resulting in year-round transmission at these areas. Previous studies (Simple et al., 2018; Tompkins and Di Giuseppe, 2015; Reiner et al., 2015; Ikeda et al., 2017) have reported malaria lagging behind rainfall at about 1 to 2 months but our study has further demonstrated that malaria season onset may lag behind rainfall only at markedly seasonal rainfall areas in Sub-Saharan Africa.

5 Conclusion

Clinical malaria case data is commonly utilized as a malariometric in examining the relationship between climate and seasonal malaria transmission in Sub-Saharan Africa. This data, on the other hand, is fraught with uncertainty due to out-of-sample generalization over geography and time, erroneous diagnosis, and under-counting due to varying health-seeking behavior and policy. As a result, in this work, we explored the applicability of high-quality EIR measurements to link rainfall and temperature seasonality to seasonal malaria outcomes in Sub-Saharan Africa. The main goal was to determine the climate variables that significantly drives malaria seasonality and their relative importance in the sub-region. Sub-Saharan Africa was first divided into four distinct climate zones namely Sahel, Guinea, WCA, and EA. The division was necessary because each zone has a unique climate conditions and therefore will have different climate implications on malaria seasonality. Applying a multi-regression statistics, pair-wise comparison and cross-correlation approaches to a $\mathrm{EIR_m}$ database gathered from publicly available field campaigns for each zone, the climate variables that explained significant variations in EIR seasonality were determined.

Findings in this study affirmed previous understanding that seasonal malaria transmission is barely impossible below 16°C or above 40°C temperature threshold (Shapiro et al., 2017; Mordecai et al., 2013). Hence, for seasonal malaria transmission to be sustained, average temperature should be well above the minimum or well below maximum threshold. While previous studies (Craig et al., 1999; Ermert et al., 2011) suggest that the monthly minimum rainfall requirement for seasonal transmission is about 80 mm, our study observed monthly maximum rainfall limit should be about 600 mm in WCA, and 400 mm in the Sahel, Guinea and EA. While rainfall and temperature were found to be significantly associated with EIR_m seasonality in the Sahel, Guinea and EA, they were not important drivers of malaria seasonality in WCA. Important drivers of malaria seasonality in WCA may be due to other factors other than climate variables. In zones characterized by elevations such as EA, topography has a significant influence on which variable is an important determinant of malaria seasonality. At markedly seasonal rainfall areas such as Sahel and EA, malaria seasonal starts one month later after the rainfall season has started. However, for zones where rainfall season is bimodal such as Guinea and WCA, there is no delay between rainfall season onset and malaria season onset.

In this study, therefore, we showed that high quality EIR_m measurements can usefully supplement established metrics for seasonal malaria by demonstrating evidence for the use of EIR to directly link the risk of humans to infectious mosquito bites to climate. The study informs our understanding of the connection between climate variables and both the malaria vector and parasite biology and how that translates into malaria seasonality in Sub-Saharan Africa. This information is key for the improvement and validation of weather-driven dynamical mathematical malaria models that directly simulate EIR. Our findings provide an understanding of geographical heterogeneous malaria risk from climate effect and support future malaria modeling and forecasting efforts. The study also supplements previous works describing clinical patterns of malaria infection and morbidity. Taking into account the seasonality of malaria management, findings in this study could lead to significant public health advantages by assisting in determining when, where, and how to use vector and parasite control strategies. It can, therefore, help stakeholders establish a robust framework for monitoring, forecasting and control of malaria.

This study does not claim to have identified all the EIR_m data available across sub-Saharan Africa. It relied on EIR_m data available in repository (Yamba et al., 2018) with details explained in (Yamba et al., 2020). The study also acknowledges that the observed EIR_m data were both spatially and temporally limited and thus unavailable for many settings (as shown if Figure 1). This limitation was unavoidable because sampling mosquitoes for the determination of EIR is both labour and cost intensive. Hence, it is very difficult to have EIR_m data available for many locations and for a long period of time. Future mosquito sampling should, therefore, focus on areas of unavailable data in order to consolidate the spatial homogeneity of available EIR_m data distribution. However, an important strength of this study is its restricted geographic and climate relevance. To our knowledge, this study is the first of its kind and also that $\mathrm{EIR_m}$ data has not been explored on such a wider scale in Sub-Saharan Africa. With the amount of $\mathrm{EIR_m}$ utilized for each climate zone, it is not anticipated that the inherent limitations may have any major adverse influence on the outcome of the study.

Acknowledgments

Profound gratitude to Katholischer Akademischer Ausländer-Dienst (KAAD) and the University of Cologne, Germany for the financial assistance.

Competing interests

The authors declare that they have no competing interests.

Authors' contributions

The work presented here was carried out collaboratively among all the authors. Edmund I. Yamba compiled the database, conducted the analysis for the figures and tables and drafted the manuscript. Leonark K. Amekudzi, Andreas H. Fink and Adrian M. Tompkins co-designed the project, supervised the analysis and co-authored the paper. Enerst O. Asare and Kingsley Badu contributed to result interpretation and co-authored the paper. All the authors proofred the paper.

References

Afrane, Y. A., Githeko, A. K., and Yan, G. (2012a). The ecology of anopheles mosquitoes under climate change: Case studies from the effects of environmental changes in east africa highlands. *Annals of the New York Academy of Sciences*, 1249:204.

Afrane, Y. A., Githeko, A. K., and Yan, G. (2012b). The ecology of anopheles mosquitoes under climate change: case studies from the effects of environmental changes in east africa highlands. *Annals of the New York Academy of Sciences*, 1249:204–210.

Asare, E. O. and Amekudzi, L. K. (2017). Assessing climate driven malaria variability in ghana using a regional scale dynamical model. *Climate*, 5(1):20.

Asare, E. O., Tompkins, A. M., Amekudzi, L. K., and Ermert, V. (2016a). A breeding site model for regional, dynamical malaria simulations evaluated using in situ temporary ponds observations. *Geospatial Health*, 11(s1):390.

Asare, E. O., Tompkins, A. M., and Bomblies, A. (2016b). A regional model for malaria vector developmental habitats evaluated using explicit, pond-resolving surface hydrology simulations. *PLoS One*, 11(3):e0150626.

Atiah, W. A., Tsidu, G. M., and Amekudzi, L. K. (2020). Investigating the merits of gauge and satellite rainfall data at local scales in ghana, west africa. *Weather and Climate Extremes*, 30:100292.

Badu, K., Brenya, R. C., Timmann, C., Garms, R., and Kruppa, T. F. (2013). Malaria transmission intensity and dynamics of clinical malaria incidence in a mountainous forest region of ghana. *MWJ*, 4:14.

Bayoh, M. N. (2001). *Studies on the development and survival of Anopheles gambiae sensu stricto at various temperatures and relative humidities*. PhD thesis, Durham University.

Beier, J. C., Killen, G. F., and Githure, J. I. (1999). A short report: Entomologic inoculation rate and plasmodium falciparum malaria prevalence in africa. *Am. J. Trop. Med. Hyg*, 61(1):109–113.

Blanford, J. I., Blanford, S., Crane, R. G., Mann, M. E., Paaijmans, K. P., Schreiber, K. V., and Thomas, M. B. (2013). Implications of temperature variation for malaria parasite development across africa. *Scientific reports*, 3(1):1–11.

Boyce, R., Reyes, R., Matte, M., Ntaro, M., Mulogo, E., Metlay, J. P., Band, L., and Siedner, M. J. (2016). Severe flooding and malaria transmission in the western ugandan highlands: implications for disease control in an era of global climate change. *The Journal of infectious diseases*, 214(9):1403–1410.

Caminade, C., Kovats, S., Rocklov, J., Tompkins, A. M., Morse, A. P., Colon-Gonzalez, F. J., Stenlund, H., Martens, P., and Lloyd, S. J. (2014). Impact of climate change on global malaria distribution. *PNAS*, 111(9):3286–3291.

Craig, M. H., Snow, R. W., and le Seur, D. (1999). A climate-based distribution model of malaria transmission in sub-saharan africa. *Parasitology Today*, 15(3):105–111.

Curran-Everett, D. (2018). Explorations in statistics: the log transformation. *Advances in physiology education*, 42(2):343–347.

Degarege, A., Fennie, K., Degarege, D., Chennupati, S., and Madhivanan, P. (2019). Improving socioeconomic status may reduce the burden of malaria in sub saharan africa: A systematic review and meta-analysis. *PloS one*, 14(1):e0211205.

Ermert, V., Fink, A. H., Jones, A. E., and Morse, A. P. (2011). Development of a new version of the liverpool malaria model. i. refining the parameter settings and mathematical formulation of basic processes based on a literature review. *Malaria journal*, 10(1):35.

Fournet, F., Cussac, M., Ouari, A., Meyer, P.-E., Toé, H. K., Gouagna, L.-C., and Dabiré, R. K. (2010). Diversity in anopheline larval habitats and adult composition during the dry and wet seasons in ouagadougou (burkina faso). *Malaria journal*, 9(1):78.

Froidurot, S. and Diedhiou, A. (2017). Characteristics of wet and dry spells in the west african monsoon system. *Atmospheric Science Letters*, 18(3):125–131.

Gething, P. W., Patil, A. P., Smith, D. L., Guerra, C. A., Elyazar, I. R. F., Johnston, G. L., Tatem, A. J., and Hay, S. I. (2011). A new world malaria map: Plasmodium falciparum endemicity in 2010. *Malaria journal*, 10(1):378.

Gleixner, S., Demissie, T., and Diro, G. T. (2020). Did era5 improve temperature and precipitation reanalysis over east africa? *Atmosphere*, 11(9):996.

Grömping, U. (2007). Relative importance for linear regression in r: the package relaimpo. *Journal of statistical software*, 17:1–27.

Hersbach, H., Bell, B., Berrisford, P., Hirahara, S., Horányi, A., Muñoz-Sabater, J., Nicolas, J., Peubey, C., Radu, R., Schepers, D., et al. (2020). The era5 global reanalysis. *Quarterly Journal of the Royal Meteorological Society*, 146(730):1999–2049.

Ikeda, T., Behera, S. K., Morioka, Y., Minakawa, N., Hashizume, M., Tsuzuki, A., Maharaj, R., and Kruger, P. (2017). Seasonally lagged effects of climatic factors on malaria incidence in south africa. *Scientific reports*, 7(1):2458.

Kar, N. P., Kumar, A., Singh, O. P., Carlton, J. M., and Nanda, N. (2014). A a review of malaria transmission dynamics in forest ecosystems. *Parasites and Vectors*, 7(265).

Kilama, M., Smith, D. L., Hutchinson, R., Kigozi, R., Yeka, A., Lavoy, G., Kamya, M. R., Staedke, S. G., Donnelly, M. J., Drakeley, C., Greenhouse, B., Dorsey, G., and Lindsay, S. W. (2014). Estimating the annual entomological inoculation rate for plasmodium falciparum transmitted by anopheles gambiae s.l. using three sampling methods in three sites in uganda. *Malaria Journal*, 13(111).

Komen, K., Olwoch, J., Rautenbach, H., Botai, J., and Adebayo, A. (2015). Long-run relative importance of temperature as the main driver to malaria transmission in limpopo province, south africa: A simple econometric approach. *EcoHealth*, 12(1):131–143.

Lowe, R., Chirombo, J., and Tompkins, A. M. (2013). Relative importance of climatic, geographic and socio-economic determinants of malaria in malawi. *Malaria journal*, 12(1):416.

Lunde, T. M., Bayoh, M. N., and Lindtjørn, B. (2013a). How malaria models relate temperature to malaria transmission. *Parasites & vectors*, 6(1):20.

Lunde, T. M., Korecha, D., Loha, E., Sorteberg, A., and Lindtjørn, B. (2013b). A dynamic model of some malaria-transmitting anopheline mosquitoes of the afrotropical region. i. model description and sensitivity analysis. *Malaria Journal*, 12(1):1–29.

Mabaso, M. L., Vounatsou, P., Midzi, S., Da Silva, J., and Smith, T. (2006). Spatio-temporal analysis of the role of climate in inter-annual variation of malaria incidence in zimbabwe. *International Journal of Health Geographics*, 5(1):20.

Mabaso, M. L. H., Craig, M., Ross, A., and Smith, T. (2007). Environmental predictors of the seasonality of malaria transmission in africa: the challenge. *Am. J. Trop. Med. Hyg.*, pages 33–38.

Manzanas, R., Amekudzi, L., Preko, K., Herrera, S., and Gutiérrez, J. (2014). Precipitation variability and trends in ghana: An intercomparison of observational and reanalysis products. *Climatic change*, 124(4):805–819.

MARA (1998). Towards an atlas of malaria risk in africa. towards an atlas of malaria transmission in africa: First technical report of the mara/arma. Technical Report 30, South African Medical Research Council, IDRC, Canada and Wellcome Trust, UK.

Markham, C. G. (1970). Seasonality of precipitation in the united states. *Ann. Ass. Am. Geogr.*, 60:593–597.

Midekisa, A., Beyene, B., Mihretie, A., Bayabil, E., and Wimberly, M. C. (2015). Seasonal associations of climatic drivers and malaria in the highlands of ethiopia. *Parasites & vectors*, 8(1):1–11.

Mordecai, E. A., Paaijmans, K. P., Johnson, L. R., Balzer, C., Ben-Horin, T., de Moor, E., McNally, A., Pawar, S., Ryan, S. J., Smith, T. C., et al. (2013). Optimal temperature for malaria transmission is dramatically lower than previously predicted. *Ecology letters*, 16(1):22–30.

Murray, C. J., Rosenfeld, L. C., Lim, S. S., Andrews, K. G., Foreman, K. J., Haring, D., Fullman, N., Naghavi, M., Lozano, R., and Lopez, A. D. (2012). Global malaria mortality between 1980 and 2010: a systematic analysis. *Lancet*, 379:413–31.

Nicholson, S. E. (2013). The west african sahel: a review of recent studies on the rainfall regime and its interannual variability. *ISRN Meteorol*, 2013:1–32.

Oses, N., Azpiroz, I., Marchi, S., Guidotti, D., Quartulli, M., and G Olaizola, I. (2020). Analysis of copernicus' era5 climate reanalysis data as a replacement for weather station temperature measurements in machine learning models for olive phenology phase prediction. *Sensors*, 20(21):6381.

Paaijmans, K. P., Blanford, S., Bell, A. S., Blanford, J. I., Read, A. F., and Thomas, M. B. (2010). Influence of climate on malaria transmission depends on daily temperature variation. *Proc Natl Acad Sci USA*, 107(33):15135–15139.

Parham, P. E. and Michael, E. (2010). Modeling the effects of weather and climate change on malaria transmission. *Environmental Health Perspectives*, 118(5):620–626.

Reiner, R. C., Geary, M., Atkinson, P. M., Smith, D. L., and Gething, P. W. (2015). Seasonality of plasmodium falciparum transmission: a systematic review. *Malaria journal*, 14(1):343.

Schneider, U., Becker, A., Finger, P., Meyer-Christoffer, A., and Ziese, M. (2018). Gpcc full data monthly product version 2018 at 0.25○: Monthly land-surface precipitation from rain-gauges built on gts-based and historical data. *GPCC: Offenbach, Germany*.

Shapiro, L. L., Whitehead, S. A., and Thomas, M. B. (2017). Quantifying the effects of temperature on mosquito and parasite traits that determine the transmission potential of human malaria. *PLoS biology*, 15(10):e2003489.

Shaukat, A. M., Bremen, J. G., and McKenzie, F. E. (2010). Using the entomological inoculation rate to assess the impact of vector control on malaria parasite transmission and elimination. *Malaria Journal*, 9(112).

Simple, O., Mindra, A., Obai, G., Ovuga, E., and Odongo-Aginya, E. I. (2018). Influence of climatic factors on malaria epidemic in gulu district, northern uganda: A 10-year retrospective study. *Malaria research and treatment*, 2018.

Sinka, M. E., Bangs, M. J., Manguin, S., Coetzee, M., Mbogo, C. M., Hemingway, J., Patil, A. P., Temperley, W. H., Gething, P. W., Kabaria, C. W., Okara, R. M., Van Boeckel, T., Godfray, H. C. J., Harbach, R. E., and Hay, S. I. (2010). The dominant anopheles vectors of human malaria in africa, europe and middle east: Occurrence data, distribution maps and bionomic precis. *Parasites and Vectors*, 3(117).

Takken, W. and Lindsay, S. W. (2003). *Ecological aspect for application of genetically modified mosquitoes*. Kluwer academic publishers, Netherlands.

Tarek, M., Brissette, F. P., and Arsenault, R. (2020). Evaluation of the era5 reanalysis as a potential reference dataset for hydrological modelling over north america. *Hydrology and Earth System Sciences*, 24(5):2527–2544.

Thompson, M. C., Mason, S. J., Phindela, T., and Connor, S. J. (2005). Use of rainfall and sea surface temperature monitoring for malaria early warning in bostwana. *Am J Trop Med Hyg*, 73(1):214–221.

Tompkins, A. M. and Di Giuseppe, F. (2015). Potential predictability of malaria in africa using ecmwf monthly and seasonal climate forecast. *Journal of applied meteorology and climatology*, 54:521–540.

Tompkins, A. M. and Ermert, V. (2013). A regional-scale, high resolution dynamical malaria model that accounts for population density, climate and surface hydrology. *Malaria Journal*, 12(65).

Tusting, L. S., Bousema, T., Smith, D. L., and Drakeley, C. (2014). Measuring changes in plasmodium falciparum transmission: precission, accuracy and cost of metrics. *Advance Parasitol*, 84:151–208.

WHO (2020). World malaria report 2020: 20 years of global progress and challenges. In *World malaria report 2020: 20 years of global progress and challenges*.

Yadav, K., Dhiman, S., Rabha, B., Saikia, P., and Veer, V. (2014). Socio-economic determinants for malaria transmission risk in an endemic primary health centre in assam, india. *Infectious diseases of poverty*, 3(1):19.

Yamba, E. I. (2016). *Improvement and validation of dynamical malaria models in Africa*. PhD thesis, University of Cologne.

Yamba, E. I., Tompkins, A. M., Fink, A. H., Ermert, V., Amelie, M. D., Amekudzi, L. K., and Briët, O. J. (2020). Monthly entomological inoculation rate data for studying the seasoanality of malaria transmission in africa. *Data*, 5(2):31.

Yamba, E. I., Tompkins, A. M., Fink, A. H., Ermert, V., Djouda, A., Amekudzi, L. K., and Briët, O. J. T. (2018). Monthly entomological inoculation rates for studying malaria transmission seasonality in Africa.

Supporting Information for "Climate drivers of malaria seasonality and their relative importance in Sub-Saharan Africa"

Edmund I. Yamba[1], Andreas H. Fink[2], Kingsley Badu[3], Ernest O. Asare[4],

Adrian M. Tompkins[5]and Leonard K. Amekudzi[1]

[1]Department of Meteorology and Climate Science, Kwame Nkrumah University of Science and Technology (KNUST), Kumasi-Ghana

[2]Institute of Meteorology and Climate Research, Karlsruhe Institute of Technology, Karlsruhe, Germany

[3]Theoretical and Applied Biology, Kwame Nkrumah University of Science and Technology, Kumasi, Ghana

[4]Department of Epidemiology of Microbial Diseases, Yale School of Public Health, Yale University, New Haven, CT, USA

[5]International Centre for Theoretical Physics, Earth System Physics, Trieste, Italy

1. Introduction

The tables provide detailed information on the study locations where mosquitoes have been collected and estimated for EIR. Geographical information for each location include: country and village where the survey took place; the longitude (lon), latitude (lat) and the elevation of the place; whether the location is rural (R) or periurban (PU) and had no permanent water body or irrigation activities. Other important information include: the year the data collection started (SY) and ended (EY), the month the data collection started (SM) and end (EM).

Corresponding author: E. I. Yamba, Department of Meteorology and Climate Science, Kwame Nkrumah University of Science and Technology, Kumasi, Ghana. Email: eiyamba@knust.edu.gh

Figure S1 shows the climate characteristics Sahel, Guinea, WCA and EA. It depicts the distinct seasonal profile of rainfall, minimum and maximum temperature for each zone.

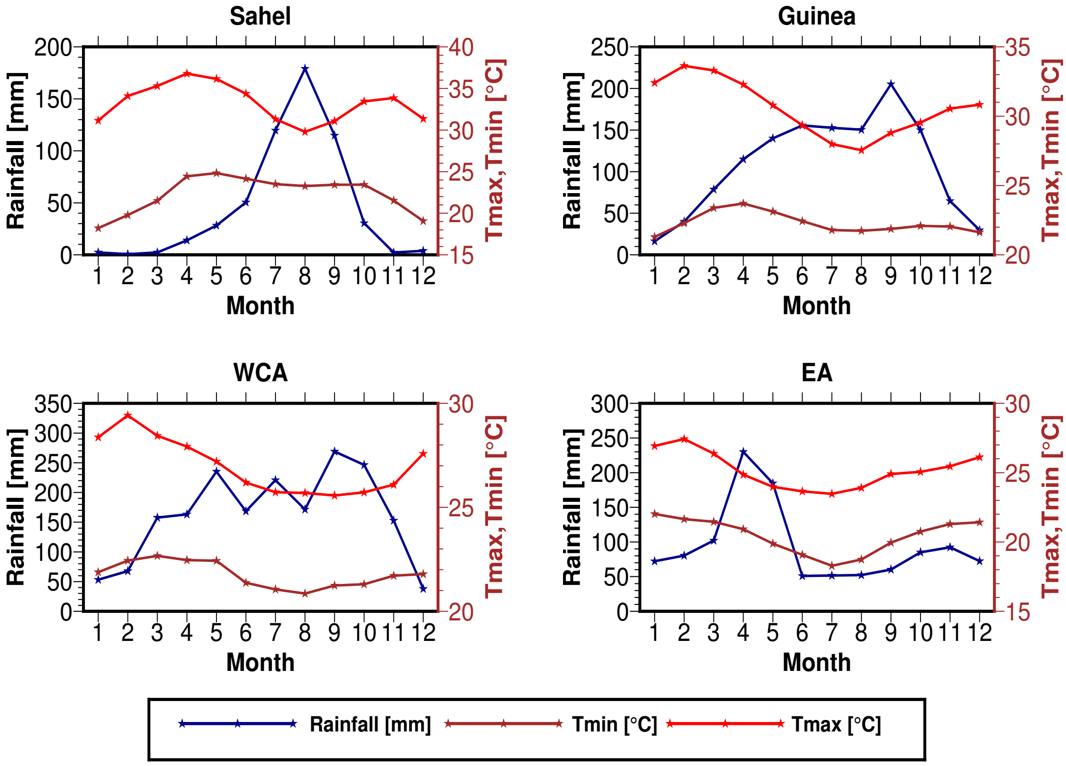

Figure S1. The monthly timeseries of RR, T_n and T_x over the difference climate zones

Table S1. Malaria EIR database locations for Sahel. Pd=population density type, SY=start year of data, EY=End year of data, SM=start month of data, EM= end month of data.

Country	site	lon	lat	elevation	Pd	Hydrology	SY	SM	EY	EM
Burkina Faso	Dande	-4.557	11.582	275	R	N	1983	01	1984	12
Burkina Faso	Koubri	-1.406	12.198	289	R	N	1984	03	1985	02
Burkina Faso	Lena	-3.98	11.28	307	R	N	1999	01	2001	12
Burkina Faso	Pabre	-1.57	12.505	303	R	N	1984	03	1985	02
Burkina Faso	Tago	-2.643	12.932	308	R	N	1983	01	1983	12
Eritrea	Adibosqual	38.39	15.42	1482	R	N	1999	01	1999	12
Eritrea	Anseba Adibosqual	38.39	15.42	894	R	N	1999	10	2000	09
Eritrea	Anseba Hagaz	37.39	15.42	894	R	N	1999	10	2000	09
Eritrea	Dasse	37.29	14.55	916	R	N	1999	01	1999	12
Eritrea	Gash Barka Dasse	37.29	14.55	610	R	N	1999	10	2000	09
Eritrea	Gash Barka Hiletsidi	36.39	15.07	610	R	N	1999	10	2000	09
Eritrea	Hagaz	38.17	15.42	883	R	N	1999	01	1999	12
Eritrea	Hiletsidi	36.39	15.07	586	R	N	1999	01	1999	12
Eritrea	Maiaini	39.09	14.49	1554	R	N	1999	01	1999	12
Ghana	KND Lowland	-1.33	10.84	212	R	N	2001	06	2002	05
Ghana	KND Rocky Highland	-1.33	10.84	212	R	N	2001	06	2002	05
Mali	Ndebougou Sector	-5.96	14.327	280	R	N	1999	04	2000	03
Mali	Molodo Sector	-6.03	14.257	280	R	N	1999	04	2000	03
Mali	Sotuba	-7.91	12.66	323	R	N	1998	01	1998	12
Senegal	Aere Lao	-14.32	16.4	13	R	N	1982	05	1983	04
Senegal	Affiniam Diagobel Tendimane	-16.24	14.28	12	R	N	1985	01	1986	12
Senegal	Barkedji	-14.88	15.28	349	R	N	1994	06	1996	05
Senegal	Boke Dialllobe	-14	16.07	28	R	N	1982	05	1983	04
Senegal	Ndiop	-16.36	15.95	6	R	N	1993	01	1996	12
Senegal	Ngayokheme	-16.43	14.53	11	R	N	1995	01	1995	12
Senegal	Takeme and Ousseuk	-16.24	14.28	21	R	N	1985	01	1986	12
Senegal	Toulde Galle	-14.48	16.53	11	R	N	1990	06	1992	05

Table S2. Malaria EIR database locations for Guinea. Pd=population density type, SY=start year of data, EY=End year of data, SM=start month of data, EM= end month of data.

Country	site	lon	lat	elevation	Pd	Hydrology	SY	SM	EY	EM
Ghana	Abotanso	-0.26	6.09	374	R	N	2004	09	2005	08
Ghana	Gyidim	-1.11	6.81	408	R	N	2003	11	2005	10
Ghana	Hwidiem	-2.35	6.93	186	R	N	2003	11	2005	10
Ghana	Kintampo	-1.73	8.05	354	R	N	2003	11	2006	10
Ghana	LowCost	-1.33	6.38	250	R	N	2003	11	2005	10
Ivory Coast	Beoue	-7.87	6.55	268	R	N	1998	04	1999	03
Ivory Coast	Bouake Dar es Salam	-5.04	7.69	325	PU	N	1991	01	1992	12
Ivory Coast	Bouake Kennedy	-5.01	7.69	351	PU	N	1991	01	1992	12
Ivory Coast	Bouake Sokoura	-5.01	7.90	361	PU	N	1991	01	1992	12
Ivory Coast	Danta	-8.16	7.02	272	R	N	1998	04	1999	03
Ivory Coast	Douandrou	-7.92	6.54	237	R	N	1998	04	1999	03
Ivory Coast	Douedy-Guezon	-7.75	6.57	266	R	N	1998	04	2000	03
Ivory Coast	Folofonkaha	-5.21	8.58	328	R	N	1996	12	1997	11
Ivory Coast	Ganse	3.9	8.617	392	R	N	2000	07	2002	06
Ivory Coast	Glopaoudy	-7.63	6.55	234	R	N	1998	04	1999	03
Ivory Coast	Kabolo	-4.99	8.19	268	R	N	1996	12	1997	11
Ivory Coast	Kafine	-5.67	9.27	322	R	N	1995	01	1995	12
Ivory Coast	Kaforo	-5.67	9.29	329	R	N	1996	12	1997	11
Ivory Coast	Kombolokoura	-5.88	9.33	366	R	N	1996	12	1997	11
Ivory Coast	Petionara	-5.12	8.43	277	R	N	1996	12	1997	11
Ivory Coast	Pohan	-7.93	6.54	249	R	N	1998	04	2000	03
Ivory Coast	Seileu	-8.17	7.10	337	R	N	1998	04	1999	03
Ivory Coast	Tai	-7.12	5.75	218	R	N	1995	07	1996	06
Ivory Coast	Tiemelekro	-4.617	6.5	91	R	N	2002	01	2003	12
Ivory Coast	Tioroniaradougou	-5.70	9.36	361	R	N	1996	12	1997	11
Ivory Coast	Zaïpobly and Gahably	-7.0	5.5	180	R	N	1995	07	1997	06
Ivory Coast	Ziglo	-7.80	6.57	256	R	N	1998	04	2000	03
Sierra Leone	Mendewa	-11.48	8.17	325	R	N	1990	01	1990	12
Sierra Leone	Nyandeyama	-11.62	8.12	118	R	N	1990	01	1990	12

Table S3. Malaria EIR database locations for WCA. Pd=population density type, SY=start year of data, EY=End year of data, SM=start month of data, EM= end month of data.

Country	site	lon	lat	elevation	Pd	Hydrology	SY	SM	EY	EM
Cameroon	Koundou	12.12	3.90	705	R	N	1997	06	1998	05
Cameroon	Ebogo	11.47	3.40	659	R	N	1991	04	1992	03
Cameroon	Ebolakounou	12.44	3.91	701	R	N	1997	06	1998	05
Cameroon	Esuke camp	9.31	4.10	279	R	N	2004	10	2005	09
Cameroon	Idenau	9.05	4.21	359	R	N	2001	08	2002	07
Cameroon	Likoko	9.31	4.39	1933	R	N	2002	10	2003	09
Cameroon	Limbe	9.18	4.03	185	R	N	2001	08	2002	07
Cameroon	Nkoteng	12.05	4.5	587	R	N	1999	02	2001	01
Cameroon	Ndogpassi	10.13	3.08	72	R	N	2011	01	2011	12
Cameroon	Tiko	9.36	4.08	182	R	N	2001	08	2002	07
Gabon	Benguia	13.52	-1.63	37	R	N	2003	05	2004	04
Gabon	Dienga	12.68	-1.87	772	R	N	2003	05	2004	04

Table S4. Malaria EIR database locations for EA. Pd=population density type, SY=start year of data, EY=End year of data, SM=start month of data, EM= end month of data.

Country	site	lon	lat	elevation	Pd	Hydrology	SY	SM	EY	EM
Burundi	Katumba	29.237	-3.317	776	R	N	1982	01	1982	12
Kenya	Asembo	34.40	-0.18	1148	PU	N	1988	03	1989	02
Kenya	Kameichiri	37.62	-0.82	1188	PU	N	2004	04	2005	03
Kenya	Kilifi	39.85	-3.62	18	PU	N	1990	12	1991	11
Kenya	Mumias	34.49	0.34	1311	PU	N	1995	05	1996	04
Kenya	Murinduko	37.45	-0.57	1311	PU	N	2004	04	2005	03
Kenya	Sokoke	39.88	-3.33	125	R	N	1990	12	1991	11
Mozambique	CdSLCMPC	32.57	-25.92	35	PU	N	1985	01	1985	12
Tanzania	Bagamoyo	38.26	-5.04	1093	R	N	1995	10	1996	09
Tanzania	Balangai	38.28	-4.56	1230	R	N	1995	10	1996	09
Tanzania	Chasimba	38.82	-6.58	36	R	N	1992	01	1992	12
Tanzania	Kisangasangeni	37.39	-3.39	759	PU	N	1994	07	1995	06
Tanzania	Kwameta	38.29	-5.08	671	R	N	1995	10	1996	09
Tanzania	Kwamhanya	38.28	-5.04	596	R	N	1995	10	1996	09
Tanzania	Magundi	38.28	-5.04	671	R	N	1995	10	1996	09
Tanzania	Mapinga	39.07	-6.60	59	R	N	1992	01	1992	12
Tanzania	Milungui	38.23	-4.45	1636	R	N	1995	10	1996	09
Tanzania	Mvuleni	37.33	-3.39	786	PU	N	1994	07	1995	06
Tanzania	Yombo	38.85	-6.59	36	R	N	1992	01	1992	12
Tanzania	Zinga	38.99	-6.52	22	R	N	1992	01	1992	12
Uganda	Apac-Olami	32.56	1.89	1053	R	N	2001	06	2002	05
Uganda	Arua-Cilio	31.02	3.11	976	PU	N	2001	06	2002	05
Uganda	Kabale villages	29.98	-1.22	1888	PU	N	1997	10	1998	09
Uganda	Kanungu Kihihi	29.70	0.59	758	R	N	2001	06	2002	05
Uganda	Kyenjojo Kasiina	30.65	0.62	1361	R	N	2001	06	2002	05
Uganda	Tororo-Namwaya	34.18	0.68	1143	PU	N	2001	06	2002	05
Zambia	Chidakwa	26.791	-16.393	1000	R	N	2005	11	2006	10
Zambia	Lupata	26.791	-16.393	1000	R	N	2005	11	2006	10

Table S5. Results of the relative importance of the meteorological predictors of $\mathbf{EIR_m}$ for locations with elevations between 501–1000 m. Variables with significant contributions are are boldfaced.

Zone	R^2 [%]	Variable	lmg [%]	First [%]	Coefficient (R)	P-value
Sahel	10.08	RR	3.20	7.07	0.2070	0.0189
		T_{max}	2.73	3.60	-4.3460	0.1300
		T_{min}	2.36	1.22	2.7780	0.2320
		T_{mean}	1.79	0.45	-0.9683	0.7490
Guinea	-	RR	-	-	-	-
		T_{max}	-	-	-	-
		T_{min}	-	-	-	-
		T_{mean}	-	-	-	-
WCA	8.96	RR	0.77	1.79	0.2630	0.1350
		T_{max}	4.89	3.71	-9.5780	0.1060
		T_{min}	0.91	0.18	-5.0120	0.6650
		T_{mean}	2.39	1.63	-9.5740	0.2330
EA	6.74	RR	0.68	0.21	-0.0951	0.6070
		T_{max}	3.02	2.34	4.6330	0.0847
		T_{min}	1.14	0.14	1.1540	0.6340
		T_{mean}	1.90	1.04	3.1700	0.2350